J Appl Electrochem (2008) 38:1485–1494
DOI 10.1007/s10800-008-9593-4

ORIGINAL PAPER

Electrochemical impedance spectroscopy investigation of spinel type cobalt oxide thin film electrodes in alkaline medium

E. Laouini · M. Hamdani · M. I. S. Pereira · J. Douch · M. H. Mendonça · Y. Berghoute · R. N. Singh

Received: 12 November 2007 / Accepted: 12 May 2008 / Published online: 28 May 2008

Abstract Spinel type Co_3O_4 thin films, for the oxygen evolution reaction (OER) in 1 M KOH, have been prepared, on stainless steel supports, using the thermal decomposition method at 400 °C. The electrochemical behaviour of the oxide film/1 M KOH interface was investigated by cyclic voltammetry and impedance techniques. The impedance measurements were carried out at different positive potentials, from the open circuit potential to a potential in the OER region and the electrical equivalent circuit, L (R_1Q_1) (R_2Q_2) (R_3Q_3) was used to fit the experimental results. At each potential, a good correlation between experimental and simulated data is found, thereby validating the proposed equivalent circuit model. The roughness factor value determined in the potential region where the charge transfer reaction is negligible is similar to that obtained by cyclic voltammetry, with a value of 70 ± 2.

E. Laouini · M. Hamdani (✉) · J. Douch · Y. Berghoute
Laboratoire de Chimie Physique, Faculté des Sciences, Université Ibn Zohr, Cité Dakhla, B.P. 8106 Agadir Maroc, Morocco
e-mail: hamdani.mohamed@gmail.com

M. I. S. Pereira · M. H. Mendonça
Centro de Ciências Moleculares e Materiais, Faculdade de Ciências da Universidade de Lisboa, Campo Grande Ed. C8, 1749-016 Lisboa, Portugal
e-mail: misp@fc.ul.pt

R. N. Singh
Department of Chemistry, Faculty of Science, Banaras Hindu University, Varanasi 221 005, India
e-mail: rnsbhu@rediffmail.com

Keywords Thin films · Oxygen evolution · Electrocatalysis · Cobalt oxide electrode · Impedance · Alkaline solution

1 Introduction

The development of highly active, stable and low-cost electrocatalysts is a major issue. Spinel-type cobalt oxide films have attracted much attention due to their excellent electrocatalytic properties towards the oxygen evolution reaction (OER) and good chemical stability in alkaline solution. Due to their low-cost, good conductivity and electrocatalytic activity for the OER, spinel cobalt oxides (e.g. Co_3O_4) have been the aim of a number of investigations [1–6].

The importance of the oxygen evolution reaction comes from the fact that it is the anodic reaction in key processes such as water electrolyses, metal electrowinning and organic electrosyntheses. However, due to its high overpotential, alkaline water electrolysis normally shows low energy efficiency. Efforts are being made to improve the reaction kinetics and lower the overpotential.

In recent years, increased application of electrochemical impedance spectroscopy (EIS) has been made to characterize electrochemical and electrocatalytic interfacial surface properties of oxide electrodes towards the OER so as to understand the solid state surface redox transitions (SSSRT). Palmas et al. [7] studied the behaviour of sol gel prepared Co_3O_4 powder electrodes by cyclic voltammetry and electrochemical impedance spectroscopy (EIS) in order to access solid-state surface redox transitions (SSSRT) which lead to the formation of active sites on the electrode surface for the OER in alkaline solutions. These authors confirmed that the kinetic parameters, Tafel slop,

exchange current density and electron transfer coefficient derived by EIS data are in good agreement with those obtained from polarisation experiments. They fitted impedance spectra using two equivalent circuits, Rs (R_1Q_1) (R_2Q_2) at low and Rs (R_1Q_1 (R_2Q_2)) at high anodic potentials. The circuit elements, (R_1Q_1) and (R_2Q_2) are attributable to the surface transitions of Co (III)/Co (II) and Co (IV)/Co (III) surface transitions, respectively, and Rs concerns the solution resistance.

Castro et al. [8] studied by EIS porous nickel–cobalt oxides prepared by cathodic electrodeposition, using an approximation in terms of a finite transmission model of conical pores linked in parallel, to evaluate the electrode active area under oxygen evolution. An electrical equivalent circuit, to fit OER impedance data, similar to that proposed by Palmas et al. [7] applies in the oxygen evolution potential region.

However, for porous oxide catalyst electrodes, the simpler and more frequently used electrical equivalent circuit to describe the characteristics of the interface is Rs (R_1Q_1) (R_2Q_2) [9, 10]. A similar model has also been proposed by Silva et al. [11] for cobalt oxide coatings on cold-rolled steel in alkaline sodium sulphate at different annealing temperatures. Below 550 °C the oxide is basically Co_3O_4 and the substrate is well protected.

For the same purpose, more recently, one of us [12] prepared Co_3O_4 and La-doped Co_3O_4 by microwave-assisted synthesis in the form of thin films on Ni substrates, exhibiting very low overpotentials for OER. Impedance measurements, using the LRs (R_1Q_1) (R_2Q_2) electrical equivalent circuit model (where L is an inductance), also confirmed the excellent electrocatalytic properties of La-doped Co_3O_4obtained by steady state polarization.

Studies on electrodeposited Co + Ni mixed oxide films through potential cycling were also investigated and characterized by EIS for oxygen evolution and the same circuit was used [13]. The OER mechanism was found to be a multi-step reaction involving one intermediate species adsorbed at the oxide surface. Other studies have used this circuit to fit the impedance data obtained with conductive metallic oxides [14–16]. Another electrical circuit, Rs L (R_1Q_1) (R_2Q_2) (R_3Q_3) has also been reported, where (R_1Q_1), (R_2Q_2) and (R_3Q_3) correspond to the capacitive and resistive contributions of the barrier layer/metal interface, the bulk barrier layer and the electrolyte/barrier layer interface, respectively [17, 18].

Some authors [15, 19] report that when SSSRT are involved in the oxidative process, a maximum in the double layer capacitance versus potential curve is generally observed at a potentia which coincides with the voltammetric peak. Other authors [20] have concluded that when an adsorption phenomenon is involved, the increasing charge results in a capacitance peak at a particular potential, which coincides with that of the voltammetric peak when the adsorption follows a Langmuir isotherm.

The ac impedance technique is a powerful tool for in situ characterization of the electrode-solution interface; it is a versatile experimental technique for non destructive characterisation of catalyst surfaces. Recently, we prepared thin films of Co_3O_4 on stainless steel by thermal decomposition of nitrate precursors and studied the physicochemical, electrochemical and electrocatalytic properties of the films towards the OER [21]. The present paper deals with an EIS study of similar thin films of the same oxide at oxidative potentials starting from the open circuit potential to the oxygen evolution potential. The objective is to obtain the OER kinetic parameters from impedance measurements and compare them with those previously obtained from polarisation curves on the same oxide [21].

2 Experimental

2.1 Oxide film preparation

The desired amount of cobalt nitrate was dissolved, in 100 mL of distilled water followed by the addition of one drop of concentrated HNO_3 to avoid precipitation of Co as cobalt hydroxide as a result of hydrolysis. All reagents were analytical grade purity. Scratched stainless steel plates with dimensions, 1 cm × 2 cm × 0.1 cm, were used as the substrate for oxide film preparation. Before use the steel plates were thoroughly washed with distilled water, ultrasonically cleaned in distilled water and absolute ethanol and then dried in air. The pre-treatment of the steel surface prior to coating is important for film adherence. The pretreated steel plates were placed in a drying oven at 60 °C and small drops of the mixed metal nitrates solution were dripped on the surface using a syringe. When the steel surface became dry, again small drops of the solution were dripped on the surface and dried. This procedure was repeated 4–5 times to cover the entire substrate surface uniformly. Finally, the coated steel plates were annealed at 400 °C for 2 h in a tubular furnace in air. Following this procedure black colored and adherent thin oxide films with loadings ranging between 2.0 and 2.4 mg cm^{-2} and 0.3–0.4 μm thick were obtained. The films had good adherence to the substrate.

2.2 Electrochemical analysis

2.2.1 Electrodes

Electrochemical studies were carried out in a conventional three-electrode single compartment glass cell. The potential of the working electrode was measured against a

saturated calomel electrode (SCE) (0.240 V vs. SHE). The SCE was connected through a KCl agar–agar salt bridge, the tip of which was placed as close as possible to the surface of the working electrode in order to minimize the solution resistance between the test and reference electrodes. The counter electrode was a platinum plate of 8 cm^2.

The electrical contact with the test electrode was made using a crocodile clip on a small strip of the plate, oxide free. The back of the electrode was isolated with an inert non conductive varnish and only a single face, with 2 cm^2, was exposed to the electrolyte. Electrochemical measurements were made in 1 M KOH (Merck) at 25 °C. The oxide electrodes were used "as prepared". The electrolyte volume was 50 mL and before use it was deaerated with N_2 for 20 min. For all the test electrodes, the open circuit potential was measured before starting the electrochemical studies.

2.2.2 *Technique and instrumentation*

In situ surface characterization and monitoring of the electrode were carried out by recording cyclic voltammograms at a sweep rate of 5 mV s^{-1} between 0 V (i.e.Voc) and 0.5 V versus SCE. In order to complement the oxide electrodes characterization impedance measurements were performed. Before the impedance measurements, polarization curves were recorded in the same potential region as used in recording the voltammograms. Impedance spectra were recorded every 100 mV in the potential range 0–0.7 V versus SCE.

The frequency range and the ac voltage amplitude employed in the investigation were 0.01–10^5 Hz and 5 mV, respectively. The electrochemical measurements were carried out using a computerized potentiostat electrochemical set (Voltalab PRZ 100 Radiometer-Analytical). Zview software was used to analyze the data. Results are displayed in the form of Bode and Nyquist plots. The impedance data were analyzed and fitted by using the software ZsimpWin.

3 Results and discussion

3.1 Cyclic voltammetry studies

Figure 1 shows the cyclic voltammogram for a Co_3O_4 electrode between the rest potential and 0.500 V versus SCE at a scan rate of 5 mV s^{-1}. This voltammogram displays a pair of redox peaks prior to the oxygen evolution reaction; the anodic peak being centered at 0.400 V versus SCE and the cathodic one at 0.350 V versus SCE. This pair of peaks is usually assigned to the solid state Co^{4+}/Co^{3+}

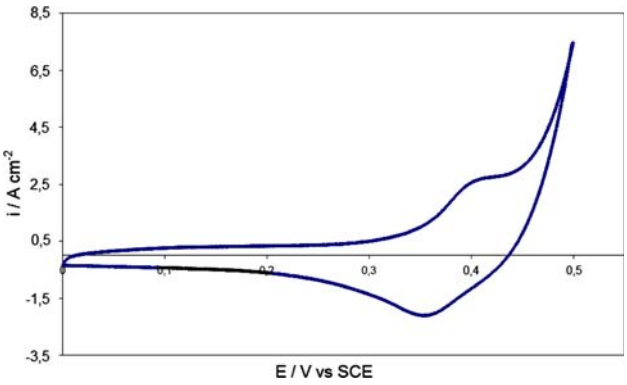

Fig. 1 Cyclic voltammogram of Co_3O_4, thin film electrodes in an N_2 deoxygenated 1 M KOH solution at a scan rate of 5 mV s^{-1}.

redox couple. The thermodynamic redox potential corresponding to the $CoOOH/CoO_2$ is E = 0.420 V versus SCE. The estimated values for the mean peak potential, Ep = (Epa + Epc)/2, and the peak potential separation, ΔEp, are 0.375 ± 0.005 V versus SCE and 0.050 ± 0.005 V, respectively. These results are in good agreement with those already reported by us [4, 5] for sprayed Co_3O_4/Ti film.

3.2 Electrochemical impedance spectroscopy (EIS)

The electrochemical impedance measurements for the Co_3O_4/1 M KOH interface were carried out at different potential values, namely 0, 0.1, 0.2, 0.3, 0.4, 0.5, 0.6, and 0.7 V at 25 °C. Before each measurement, the electrode was allowed to equilibrate at each applied dc potential. Impedance data were displayed in the form of Nyquist, Bode and admittance plots. Representative data, obtained at E = 0, 0.4, 0.5 and 0.7 V are given in Fig. 2–5. Each complex-plane diagram (Nyquist) is characterized by three distinct regions, low, intermediate and high frequency regions. However, the features of all the curves are similar, only at intermediate and high frequencies, regardless of the applied dc potential. At high frequencies, the influence of inductance on impedance predominates and increases with increasing frequency. This inductance is not associated with the electrode process, but is a contribution from the cell connections and their interaction with the surroundings [22]. At intermediate frequencies, all the curves show a depressed semicircle.

At low frequencies, and for E ≤ 0.4 V (prior to the O_2 evolution region), the sloping line on the Nyquist plots indicates that the Co_3O_4/1 M KOH interface exhibits capacitive behaviour. This may be caused by diffusion of the charge species (H^+/OH^-) into the oxide film through defects and pores [23, 24]. The capacitive behaviour of the electrode/electrolyte interface at low frequencies is common in the case of ion intercalation into an inorganic/polymer

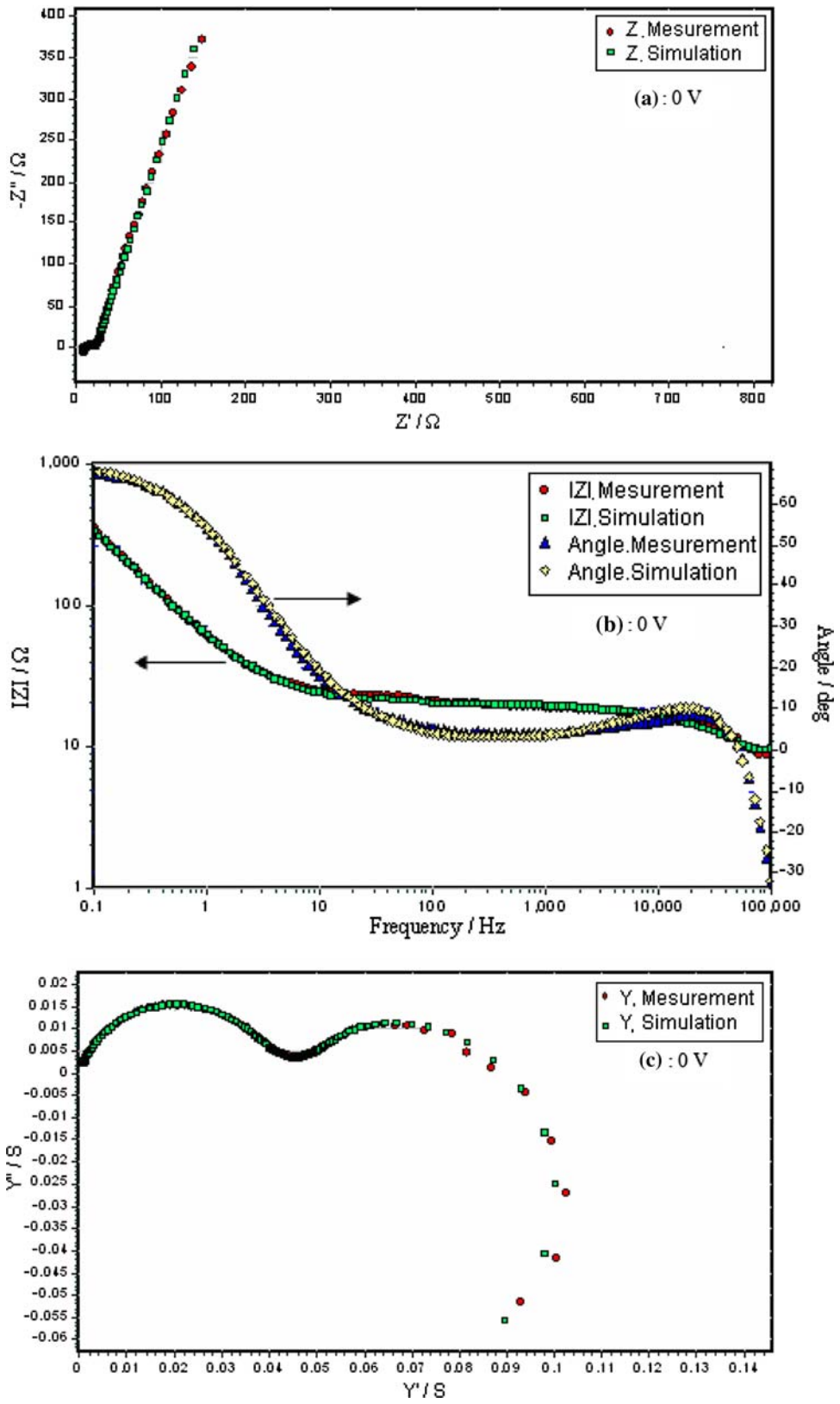

Fig. 2 Complex impedance (**a**) Nyquist, (**b**) Bode and (**c**) admittance plots, for Co_3O_4 in 1 M KOH, E = 0 V versus SCE. Experimental and simulated results

matrix [25]. In contrast, when E ≥ 0.5 V (in the O_2 evolution region), the low frequency end of the Nyquist plot gives a semicircle, the diameter of which decreases with increasing E (or overpotential, η). Thus, the formation of a potential dependent semicircle at E ≥ 0.5 V in the low frequency region can be ascribed to the OER. A similar

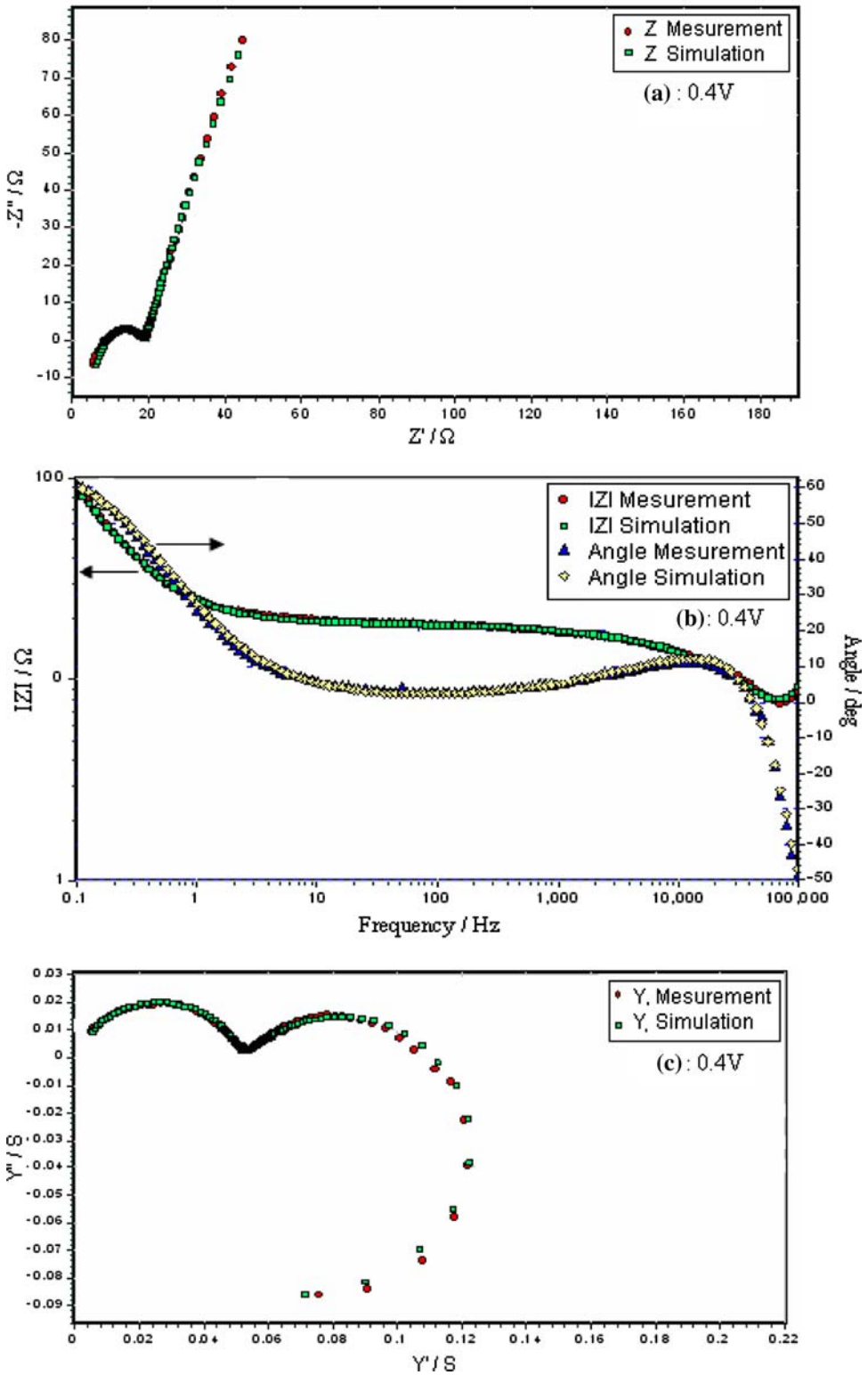

Fig. 3 Complex impedance (**a**) Nyquist, (**b**) Bode and (**c**) admittance plots, for Co_3O_4 in 1 M KOH, E = 0.4 V versus SCE. Experimental and simulated results

diagram was reported for the Co_3O_4 electrode under oxygen evolution [7].

Based on the experimental observations, a common electrical equivalent circuit composed of three resistive/capacitive elements in series, with circuit description code (CDC), LRs (RC) (RC) (RC), was proposed to compute the experimental data. The fitting procedure showed that the best agreement between the experimental and simulated data was obtained when a constant phase element (CPC) was used instead of a pure capacitance, as shown in Fig. 6.

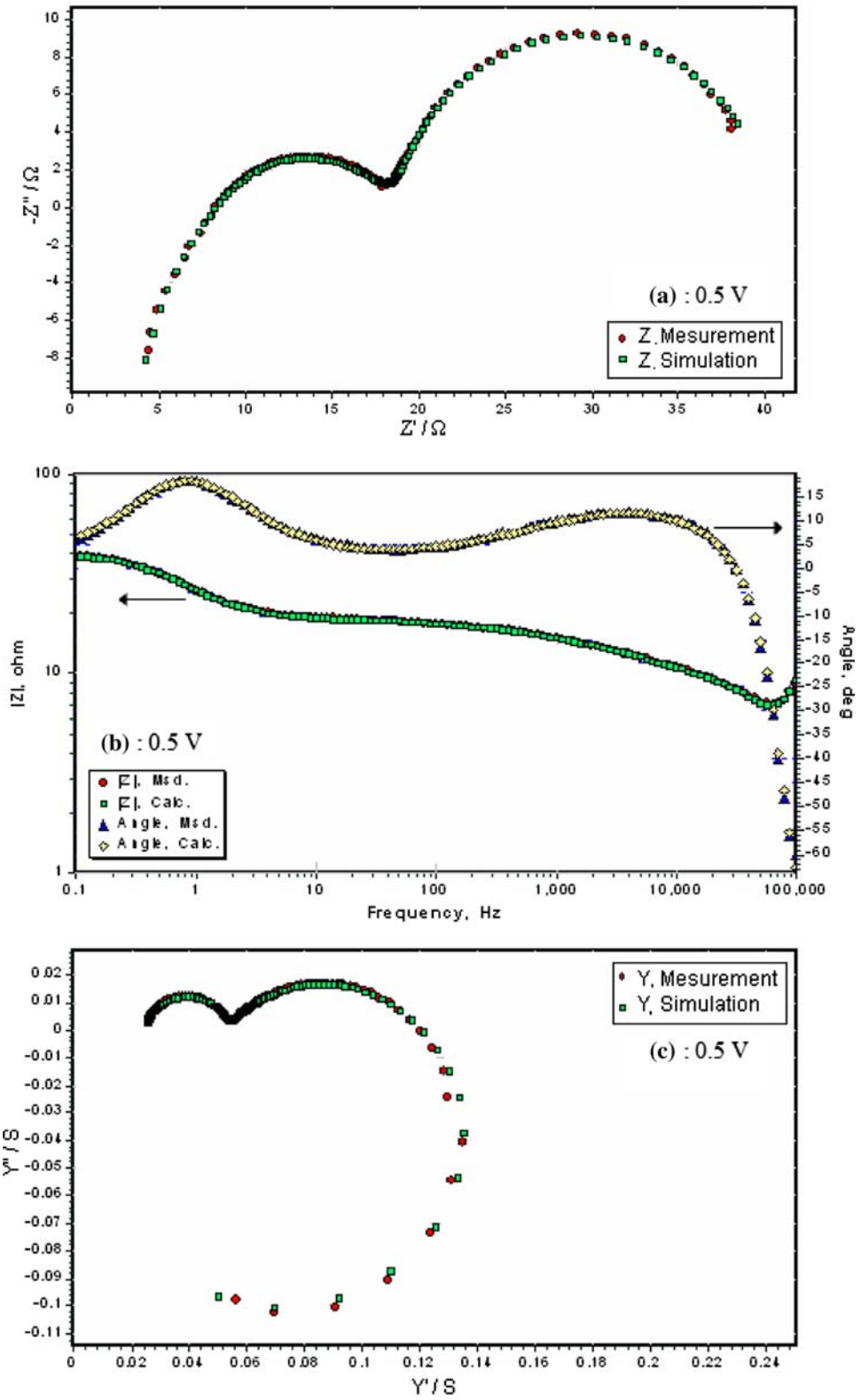

Fig. 4 Complex impedance (**a**) Nyquist, (**b**) Bode and (**c**) admittance plots, for Co_3O_4 in 1 M KOH, E = 0.5 V versus SCE. Experimental and simulated results

The EI spectra obtained from the proposed circuit model agree reasonably well with the experimental curves as shown in Figs. 2–5b. Chi-square (χ^2) values of the order of 10^{-4} were obtained, which are quite reasonable for the validity of a model. Estimates of the circuit parameters of the electrical equivalent circuit are displayed in Table 1.

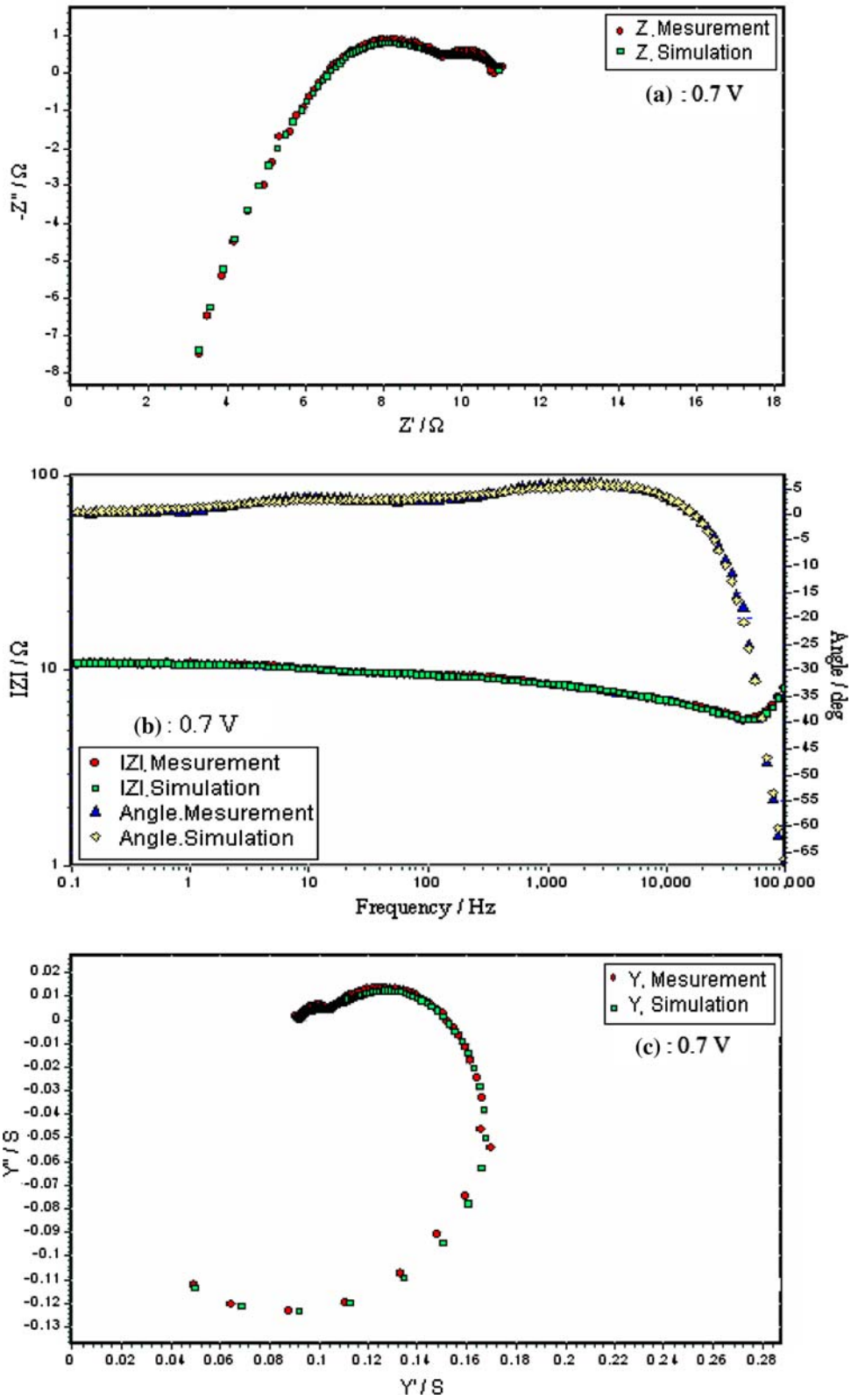

Fig. 5 Complex impedance (**a**) Nyquist, (**b**) Bode and (**c**) admittance plots, for Co_3O_4 in 1 M KOH, E = 0.7 V versus SCE. Experimental and simulated results

The time constants, τ_1, τ_2, and τ_3 corresponding to each sub circuit, namely (R_1Q_1), (R_2Q_2) and (R_3Q_3) have also been estimated at the different applied potentials using the relation,

$$\tau^n = R \cdot Q \quad (1)$$

and the values are also given in Table 1.

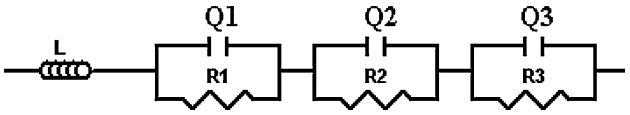

Fig. 6 Equivalent electrical circuit used to fit the experimental data of EIS

Table 1 shows that τ_1 for the resistive/ capacitive sub-circuit (R_1Q_1) is the lowest and the R_1 and Q_1 values show a slight variation with potential. Therefore, (R_1Q_1) can be assigned to the properties of the bulk oxide; R_1 being the resistance of the oxide film. The decrease in R_1, particularly at $E > 0.3$ V, can be ascribed to the formation of a high conductivity oxidized CoOOH phase [7] from the Co (III) phase. Furthermore, n_2 values are close to 0.5, while n_3 values are close to 1. At $E \leq 0.4$ V, the Nyquist plots are capacitive type at low frequencies, as shown in Fig. 7. This shows that at low frequencies there is the establishment of a transition between semi-infinite Warburg ($n_2 = 0.5$) and finite Warburg ($n_3 = 1$). Similar semi-infinite-finite Warburg transition regimes are frequently found in the literature for ion intercalation in a polymer matrix [26–28]. Thus, the sub circuits (R_2Q_2) and (R_3Q_3) represent a diffusion controlled process; that is, the migration of H^+/OH^- into the oxide matrix and charging of the double layer particles at potentials prior to the oxygen evolution region. However, the semicircle corresponding to the oxide/solution interface is not apparent in the EI spectrum, presumably due to the strong influence of the ion diffusion process in the oxide matrix. Furthermore, the solution resistance is practically $<2\ \Omega$, but the estimated values of Rs are of the order of 10^{-6}–$10^{-7}\ \Omega$ and so the final data simulation was carried without using Rs in the equivalent circuit, as shown in Fig. 6. This may be due to the dominance of inductance in the high frequency region.

On the other hand, for $E \geq 0.5$ V (a potential in the oxygen evolution region), the subcircuit (R_3Q_3) is found to be strongly influenced by the applied potential. Moreover

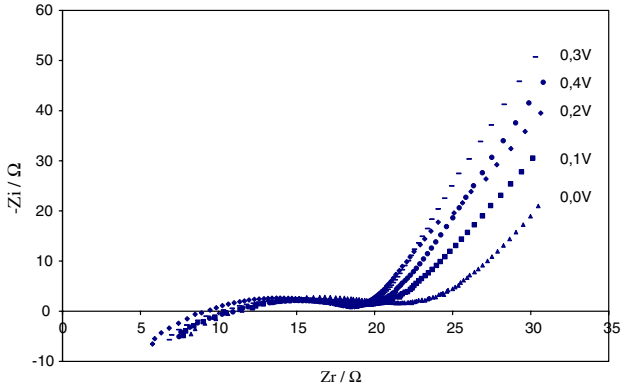

Fig. 7 Experimental Nyquist diagram for Co_3O_4 in 1 M KOH, at different potentials. Applied electrode potentials are given on the diagram

the observed capacitive behavior of the Nyquist curve at lower potentials ($E \leq 0.4$ V) becomes a semicircle. Thus, (R_3Q_3) at $E \geq 0.5$ V can be attributed to the OER and hence R_3 represents the charge transfer resistance and Q_3 the double layer capacitance in the oxygen evolution region.

The R_3 values shown in Table 1 decrease exponentially with applied potential. Values of the apparent current density (i) at different potentials were estimated using the relation (2) [7],

$$R_{ct} = RT/nFi \quad (2)$$

where R, T, n, F and i are the molar gas constant (J mol^{-1} K^{-1}), temperature (K), number of electrons involved in the reaction, (4 in the present case), Faraday constant and the apparent current density (A cm^{-2}), respectively. The apparent current density values, thus estimated, were found to be 3.0, 16.7 and 55.6 $\times$ 10^{-4} A cm^{-2} at E = 0.5, 0.6 and 0.7 V, respectively. The plot of E versus log i produced a straight line with a slope of $\sim$156 mV (Fig. 8). A similar value was by us obtained recently for the same system using steady state anodic polarization curves without any

Table 1 Estimates of the circuit parameters for the Co_3O_4 electrodes in 1 M KOH at high anodic potential

E (VSCE)	10^5 L (H cm^2)	R_1 (Ω cm^2)	10^6 Q_1 (S-s^n cm^2)	n_1	$10^6\tau_1$ (s)	R_2 (Ω cm^2)	10^4 Q_2 (S-s^n cm^2)	n_2	$10^5\tau_2$ (s)	R_3 (Ω cm^2)	10^3 Q_3 (S-s^n cm^{-2})	n_3	τ_3 (s)	Rf = C/60
0.00	1.91	17.8	1.34	0.82	2.30	9.3	95.33	0.34	80.35	3753	3.69	0.85	22.02	62
0.10	1.88	16.0	1.22	0.83	2.12	6.3	53.21	0.40	20.58	4041	4.22	0.83	30.49	70
0.20	1.84	14.6	1.40	0.83	2.24	7.4	61.59	0.35	14.72	4124	4.28	0.88	26.11	71
0.30	1.83	13.9	2.97	0.78	2.40	7.0	44.04	0.36	6.36	2446	6.95	0.80	34.52	–
0.40	1.84	8.8	2.73	0.82	2.33	10.9	5.30	0.46	1.35	902.3	18.0	0.86	25.57	–
0.50	2.0	7.8	0.45	0.95	1.81	11.1	4.10	0.57	7.79	21.4	15.42	0.80	0.25	–
0.60	2.11	8.0	0.35	0.98	2.16	10.6	4.77	0.59	12.83	3.9	18.66	0.94	0.06	–
0.70	1.57	4.8	0.49	1	2.35	3.2	6.43	0.66	8.50	1.2	24.81	0.90	0.02	–

L, R_1, R_2, Q_1, Q_2 stand for inductance, solution resistance, resistance of the oxide film, charge transfer resistance constant phase element, double layer capacitance, respectively. R_3Q_3 represent the diffusional controlled process

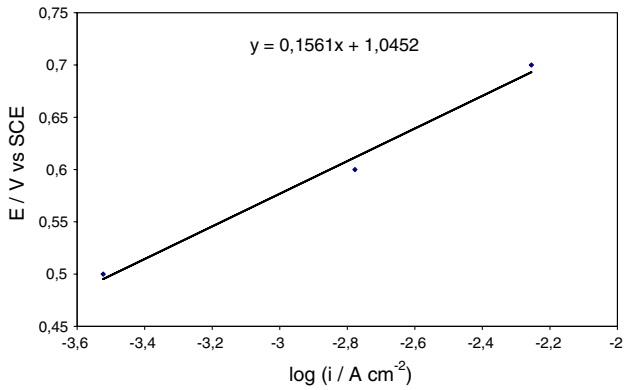

Fig. 8 Plot of log i versus potential from the formula (2) given in text

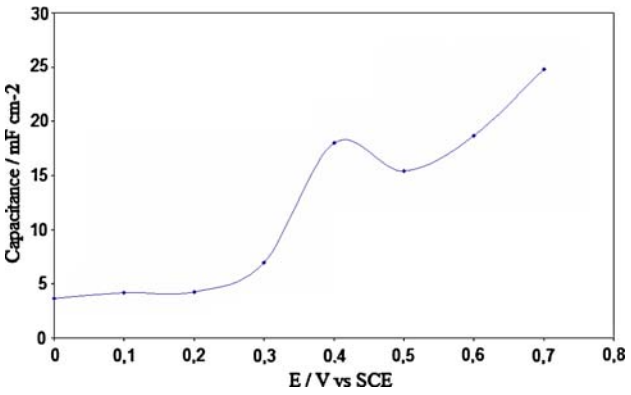

Fig. 9 Double layer capacitance of Co_3O_4 electrode as function of potential

Ohmic drop correction in the potential range between 0.5 and 0.7 V versus SCE [21]. Very recently, Palmas et al. [7], in a similar study for the system Co_3O_4/1.75 M NaOH, obtained a value for the Tafel slope of 189 mV, which is somewhat higher than that obtained in the present work.

From the data shown in Table 1, a plot of Cdl (Q_3) versus E was constructed, as shown in Fig. 9. This curve presents a similar trend to the voltammogram presented in Fig. 1. The observed maximum capacitance appears around 0.4 V which corresponds to the voltammetric peak potential. Similar Cdl versus E curves were also reported in the case of perovskite electrodes in alkaline medium by Bockris and Otagawa [29, 30]. The rising part of the curve may be due to modifications of the double layer as a result of the oxidation of Co (III) to Co (IV). Furthermore, it is known that the formation of the redox couple Co (III)/Co (IV) is a quasi-reversible diffusion controlled process. The low rate of this transition can be attributed to the slow diffusion of OH^- inside the pores. Due to this, Q_3 values are found to increase exponentially with the applied potential (0.2–0.4 V).

The roughness factor (R_F) given in Table 1 was calculated at lower potentials using the relation [31], "The observed C_{dl} of the test electrode/C_{dl} of the smooth oxide surface (60 μF cm^{-2})" and found to be 70 ± 1 for $E = 0.10$ and 0.20 V. Previously a value of 79 was estimated by us from EIS data for the same system in the same conditions [21].

A lower value, 62, was estimated for $E = 0.0$ V. This value is in good agreement with that obtained by us, 59 ± 3, at the same potential by cyclic voltammetry in the double layer region [21]. Similar values are also reported for the sprayed cobalt oxide in thin film form [4].

4 Conclusion

The electrochemical behaviour of cobalt oxide thin films was examined in 1 M KOH, in the oxidative potential range, and ac impedance was used to check and model the oxide electrode- solution interface. The electrical equivalent circuit, L (R_1Q_1) (R_2Q_2) (R_3Q_3) was used in the potential region between the open circuit and oxygen evolution, i.e. from 0 to 0.7 V. At each potential, a good correlation between experimental and simulated data is found, thereby validating the proposed equivalent circuit model. The roughness factor determined in the potential region where the charge transfer reaction is negligible is similar to that obtained by cyclic voltammetry, having a value of 70 ± 2.

Acknowledgements The authors gratefully acknowledge support of this work by CNRST (Maroc) and GRICES (Portugal) under a Research Convention project.

References

1. Trasatti S, Lodi G (1980) In: Trasatti S (ed) Electrodes of conductive metallic oxides, Part B. Elsevier, Amsterdam, p 521 and references therein
2. Tarasevich MR, Efremov (1980) In: Trasatti S (ed) Electrodes of conductive metallic oxides, Part B. Elsevier, Amsterdam, p 221 and references therein
3. Trasatti S (1994) In: Lipkowski J, Ross PN (eds) Electrochemistry of novel materials. VCH publishers Inc., New York, p 207 and references therein
4. Hamdani M, Pereira MIS, Douch J, Ait Addi A, Berghoute Y, Mendonça M. H (2004) Electrochim Acta 49:1555
5. Singh RN, Hamdani M, Koenig JF, Chartier P (1990) J Appl Electrochem 20:442
6. Singh RN, Koenig JF, Poillerat G, Chartier P (1990) J Electrochem Soc 137:1408
7. Palmas S, Ferrara F, Vacca A, Mascia M, Polcaro AM (2007) Electrochim Acta 53:400
8. Castro EB, Real SG, Pinheiro Dick LF (2004) Int J Hydrogen Energy 29:255
9. Alves VA, Da Silva LA, Boodts JFC (1998) Electrochim Acta 44:1525
10. Shieh DT, Hwang BJ (1993) Electrochim Acta 38:2239

11. Silva GC, Fugivara CS, Tremiliosi Filho G, Sumodjo PTA, Benedetti AV (2002) Electrochim Acta 47:1883
12. Singh RN, Mishra D, Anindita, Sinha ASK, Singh A (2007) Electrochem Commun 9:1369
13. Wu G, Li N, Zhou D-R, Kurachi M, Xu B-Q (2004) J Solid State Chem 177:3682
14. Hu JM, Meng HM, Zhang JQ, Cao CN (2002) Corr Sci 44:1655
15. Da Silva LA, Alves VA, Da Silva MAP, Trasatti S, Boodts JFC (1997) Electrochim Acta 42:271
16. Da Silva LM, De Faria LA, Bootd JFC (2002) J Electroanal Chem 532:141
17. Priyantha N, Jayaweera P, Macdonalt DD, Sun A (2004) J Electroanal Chem 572:409
18. Clerc C, Alkire RC (1989) In: Smyrl WH, Macdonald DD (eds) Proceedings of the symposium on transient techniques in: corrosion science and engineering, Proceedings, vol 89–1, p 57
19. Lassali TAF, Boodts JFC, Bulhoes LOS (1999) Electrochim Acta 44:4203
20. Lasia A (2002) In: Conway BE, White RE (eds) Modern aspect of Electrochemistry, vol 35. Kluwer Academic/Plenum Publishers, New York, p 1
21. Laouni E, Hamdani M, Pereira MIS, Douch J, Mendonça MH, Berghoute Y, Singh RN, Int J Energy (submited)
22. Bockris JO'M, Reddy AKN, Gamboa-Aldeco M (2000) In: Modern Electrochemistry, vol 2A, 2nd edn. Kluwer Academic/Plenum Publishers, New York, p 1132
23. Singh RN, Malviya M, Anindita, Sinha ASK, Chartier P (2007) Electrochim Acta 52:4264
24. Singh NK, Tiwari SK, Anitha KL, Singh RN (1996) J Chem Soc Faraday Trans 92:2397
25. Singh RN, Singh NK, Singh JP, Balaji G, Gajbhiye NS (2006) Int J Hydrogen Energy 31:701
26. Singh RN, Malviya M, Chartier P (2007) J New Mat Electrochem Syst 10:181
27. Penner RM, Martin CR (1989) J Phys Chem 93:984
28. Naoi K, Ueyama K, Osaka T, Smyrl WH (1990) J Electrochem Soc 137:494
29. Bockris JO'M, Otagawa T (1984) J Electrochem Soc 131(2):290
30. Bockris JO'M, Otagawa T (1983) J Phys Chem 87:2960
31. Levine S, Smith AL (1971) Discuss Faraday Soc 52:290